

7N-34
359029

NASA

MEMORANDUM

HEAT TRANSFER IN THE TURBULENT INCOMPRESSIBLE

BOUNDARY LAYER

II - STEP WALL-TEMPERATURE DISTRIBUTION

By W. C. Reynolds, W. M. Kays, and S. J. Kline
Stanford University

NATIONAL AERONAUTICS AND
SPACE ADMINISTRATION

WASHINGTON

December 1958

101

102

103

NATIONAL AERONAUTICS AND SPACE ADMINISTRATION

MEMORANDUM 12-2-58W

HEAT TRANSFER IN THE TURBULENT INCOMPRESSIBLE BOUNDARY LAYER

II - STEP WALL-TEMPERATURE DISTRIBUTION

By W. C. Reynolds, W. M. Kays, and S. J. Kline

SUMMARY

Heat-transfer rates and temperature profiles for the turbulent incompressible flow of air over a flat plate with a stepwise temperature distribution (unheated starting length) were measured for a variety of step positions at Reynolds numbers up to 3.5×10^6 . Comparison of the data with existing heat-transfer analyses indicates that an improved analysis is needed. An integral analysis is made that agrees very well with the data and allows a simple correction for the unheated starting length. In addition, a differential analysis is made that allows prediction of the temperature profiles from the velocity profiles, and good agreement with experimental profiles is obtained.

INTRODUCTION

This report is the second of a series of four covering a three-year investigation of heat transfer in the turbulent incompressible boundary layer with arbitrary wall temperature (see ref. 1). The first report describes the experimental apparatus and presents results of experiments with constant wall temperature (ref. 2). Results of experiments and analyses for a step temperature distribution are presented herein. In part III the step-function analysis is used to predict heat-transfer rates for several cases of variable wall temperature, and the predictions are compared with experimental data (ref. 3). A simple method for handling arbitrary wall-temperature problems is presented. Part IV presents an analysis of the effect of the location of the transition point on heat transfer in the turbulent boundary layer and compares the results with experimental data (ref. 4).

The problem of heat transfer from a flat plate with a stepwise temperature distribution is of interest for two reasons. The "unheated starting length" problem is in itself of interest; but more important, the step temperature distribution provides the basis for analysis of

problems involving more complex arbitrary wall-temperature distributions by use of superposition (ref. 3). Accurate analyses of the problem of step temperature distribution and experimental confirmation of these analyses are therefore of considerable importance. Prior to the present investigation, the only measurements of local heat-transfer coefficients with a step temperature distribution were those of Scesa (ref. 5). These data compare favorably with the analyses of Seban (ref. 5) and Rubesin (ref. 6) over the range attainable with Scesa's experimental apparatus. However, this range was limited by the size of his test plate. The data presented in the present report agree with the existing analyses in the range of Scesa's data but depart significantly from the analyses elsewhere. The largest departure occurs close to the discontinuity in the wall temperature, and this is the most critical region, with respect to both departure from isothermal performance and use in superposition solutions of more general problems. Thus an improved analysis is very desirable.

The integral analysis presented in this report represents an improvement over the former analyses in that the number of approximations has been reduced. The analysis involves assumption of the forms of the velocity and temperature profiles and an assumption about the mechanism of heat transfer. Use of the energy integral equation then leads to a differential equation for the thermal boundary-layer thickness which, upon solution, allows calculation of the heat-transfer rates. This analysis is in excellent agreement with both the present data and all other previous data known.

As just noted, it is necessary in an integral analysis to assume the shape of both the velocity and temperature profiles. In the present analysis, as in most such analyses, the two profiles have been assumed to be similar in shape. However, the velocity and temperature profiles in the boundary layer just downstream of a step in the wall temperature were carefully measured in the present investigation and were found to be dissimilar in this region. If the velocity profile alone is assumed, the differential energy equation of the boundary layer may then be solved in detail. This solution yields the temperature profile of the boundary layer downstream of the step in wall temperature. This analysis is referred to as the differential analysis and is presented in detail in this report. The results of the differential analysis and the measured temperature profiles agree well, and the heat-transfer predictions are in reasonable agreement with the experimental data.

The present integral and differential analyses are restricted to fluids having Prandtl numbers of unity, but should be adequate for fluids with Prandtl numbers near unity. Recently Ferrari made a similar differential analysis in which he included the effect of Prandtl number and compressibility (ref. 7). This represents a considerable

extension beyond the present analyses but is extremely complicated. However, if the flow is incompressible, Ferrari's result reduces to the result of the integral analysis for any Prandtl number. It therefore appears that the assumption of Prandtl number of unity does not seriously limit the analyses presented herein. It is felt that the present analyses are useful because of their simplicity and that they adequately represent the heat-transfer rates and temperature profiles.

An essential feature of the integral analysis is a unique method of handling the shear stress and heat flux at the wall. Although profiles having infinite gradients at the wall are employed, turbulent viscosities and conductivities are constructed so that the wall shear and heat flux are finite and have their correct values. The idea of using a velocity profile with an infinite gradient at the wall is also employed in the differential analysis. This technique eliminates the need for separate consideration of a laminar sublayer and greatly simplifies the analyses.

This investigation was carried out at Stanford University under the sponsorship and with the financial assistance of the National Advisory Committee for Aeronautics.

SYMBOLS

a	$(m + 3)/(m + 2)$
C_f	friction factor, $\tau_w/(\rho u_\infty^2/2)$
C_n	expansion coefficients
c_p	specific heat at constant pressure, Btu/(lb)(°F)
$F(a,b;c;x)$	hypergeometric function, $1 + \frac{ab}{c} \frac{x}{1!} + \frac{a(a+1)(b+1)}{c(c+1)} \frac{x^2}{2!} + \dots$
$F(a,b;c;l)$	hypergeometric function, $\frac{\Gamma(c)\Gamma(c-a-b)}{\Gamma(c-a)\Gamma(c-b)}$
G	free-stream mass velocity, ρu_∞ , lb/(hr)(sq ft)
h	convective heat-transfer coefficient, $q_w''/\Delta t_m$
k	thermal conductivity of fluid, Btu/(hr)(ft)(°F)
L	length of plate, ft

l	unheated starting length, ft
M	$m/(m+1)(m+2)$
m	parameter in velocity and temperature profiles, dimensionless
Nu	local Nusselt number, hx/k
Nu_m	mean Nusselt number over heated portion of plate
Pr	Prandtl number, $\mu c_p/k$
q''_{bl}	heat flux in boundary layer, $Btu/(hr)(sq\ ft)$
q''_w	heat flux at wall, $Btu/(hr)(sq\ ft)$
Re_l	Reynolds number based on unheated starting length, Gx/μ
Re_x	flow Reynolds number, Gx/μ
Re_δ	Reynolds number based on δ , $G\delta/\mu$
St	local Stanton number, h/Gc_p
St_m	mean Stanton number over heated portion of plate
St_T	local Stanton number for isothermal plate, $f(Re_x; Pr)$
T	absolute temperature, $^{\circ}R$
T_w	absolute wall temperature, $^{\circ}R$
T_∞	absolute free-stream temperature, $^{\circ}R$
Δt	$t_w - t_\infty$, $^{\circ}F$
t_{bl}	temperature in boundary layer, $^{\circ}F$
t_m	mean temperature of heated strip, $^{\circ}F$
Δt_m	$t_m - t_\infty$, $^{\circ}F$
t_w	wall temperature, $^{\circ}F$

t_{∞}	free-stream temperature, °F
u	velocity in x-direction, ft/sec
u_{∞}	free-stream velocity, ft/sec
v	velocity in y-direction, ft/sec
w	$\ln \xi$, dimensionless
x	distance from leading edge, ft
y	distance from plate, ft
z	u/u_{∞}
$\Gamma(x)$	gamma function, $\int_0^{\infty} e^{-z} z^{x-1} dz = (x-1)!$
δ	thickness of hydrodynamic boundary layer, ft
δ_T	thickness of thermal boundary layer, ft
δ_T^*	conduction thickness, $\int_0^{\delta_T} (1 - \theta) dy$, ft
ϵ_H	eddy diffusivity for heat, sq ft/hr
ϵ_M	eddy diffusivity for momentum, sq ft/hr
ζ	z^{m+2}
η	y/δ
θ	dimensionless temperature, $(t_w - t_{bl})/(t_w - t_{\infty})$
λ_n	eigenvalue
μ	viscosity of fluid, lb/(hr)(ft)
ν	kinematic viscosity, μ/ρ , sq ft/hr
ξ	x/l

ρ	fluid density, lb/cu ft
σ	variable of integration
τ_{bl}	shear stress in boundary layer, lb/sq ft
τ_w	shear stress at wall, lb/sq ft

ANALYSIS

Summary of Analyses

The problem of turbulent heat transfer from a flat plate with a step temperature distribution (unheated starting length) has been treated approximately in a number of ways. The results of the analyses can, in general, be put in the form

$$\frac{St}{St_T} = f\left(\frac{l}{x}\right) \quad (1)$$

where St_T represents the local Stanton number for heat transfer from a plate at constant temperature. The function $f(l/x)$ thus represents a correction that may be applied to any suitable expression for the heat transfer from an isothermal surface. Reference 2 shows that the heat-transfer - momentum-transfer analogy of von Kármán (ref. 8) may be combined with the friction analysis of Schultz-Grunow (ref. 9) to give

$$St_T = \frac{1.60(\ln Re_x)^{-2.58}}{1 + 1.26(\ln Re_x)^{-1.29} [5Pr + 5 \ln(5Pr + 1) - 14]} \quad (2)$$

This expression is felt to be the best available at the present time for turbulent incompressible flat-plate heat transfer. For air, having Prandtl number 0.7, reference 2 shows that equation (2) may be represented in the range $10^5 < Re_x < 10^7$ by

$$St_T Pr^{0.4} = 0.0296 Re_x^{-0.2} \left(\frac{T_w}{T_\infty}\right)^{-0.4} \quad (3)$$

Equation (3) represents a modification of the familiar Colburn analogy (ref. 10). In using equation (3), the fluid properties appearing in the Stanton, Prandtl, and Reynolds numbers are to be evaluated at the free-stream static temperature; the factor $(T_w/T_\infty)^{-0.4}$ corrects for the

effects of temperature-dependent fluid properties. Equation (3) is much simpler than the von Kármán result (2), and therefore is useful for computation purposes.

A first approximation to the step temperature distribution problem can be obtained if the thermal effects are assumed independent of the hydraulic effects, in which case the heat-transfer rate can be determined directly from equation (3) by forming the Reynolds number with the distance $x - l$ instead of with x . This results in

$$\frac{St}{St_T} = \left[1 - \left(\frac{l}{x} \right) \right]^{-1/5} \quad (4)$$

A second approximation was proposed by Rubesin (ref. 6), who attempted to separate the thermal and hydraulic effects in a semiempirical manner. Rubesin assumed $1/7$ -power velocity and temperature profiles and, using the energy integral equation of the boundary layer, arrived at a differential equation between δ_T and x which, strictly speaking, applies only if the plate is at constant temperature. His differential equation contained a parameter m with which he proposed to separate thermal and hydraulic effects. In comparing his result with the limited data of Scesa (ref. 5), he chose the parameter m to be zero. His final result may be put in the form

$$\frac{St}{St_T} = \left[1 - \left(\frac{l}{x} \right)^{39/40} \right]^{-7/39} \quad (5)$$

Seban (ref. 5) used a $1/7$ -power velocity profile and a temperature profile that was linear near the wall. He "patched" the linear portion to the $1/7$ -power profile in the outer portion of the boundary layer. Then, by using the energy integral equation, Seban arrived at the following result:

$$\frac{St}{St_T} = Pr^{-2/9} \left[1 - \left(\frac{l}{x} \right)^{9/10} \right]^{-1/9} \quad (6)$$

Except for the Prandtl number dependency, this result is identical with the integral analysis presented in the present work. One would expect that, well downstream of the step, the effect of the step should die out, and St/St_T should approach unity. Thus the factor $Pr^{-2/9}$ gives an improper limiting behavior for $x \rightarrow \infty$. This erroneous Prandtl number dependency in Seban's solution is a result of his "patching" of the temperature profile.

In using integral methods, there is always a problem as to what to use for the value of the heat flux at the wall (see eq. (16)). Rubesin in effect modified the isothermal value, while Seban used the slope of the temperature profile in his laminar sublayer. The latter approach is certainly more desirable, but leads to the introduction of an incorrect dependency on Prandtl number. In the present integral analysis, this term is evaluated by a limiting procedure as the product of the slope of a power profile (which is infinite at the wall) with an eddy diffusivity (which is made zero at the wall in such a manner that the shear stress and heat flux have their correct values). Then, after assuming $1/m$ -power velocity and temperature profiles, one obtains

$$\frac{St}{St_T} = \left[1 - \left(\frac{l}{x}\right)^{4(m+2)/5(m+1)} \right]^{-1/(m+2)} \quad (7)$$

For $m = 7$ this result is similar to Seban's but does not have the erroneous Prandtl number dependency. Equation (7) with $m = 7$ is in excellent agreement with the present data, and is recommended as the best step temperature distribution analysis.

The chief objection to the integral methods is that the forms of the velocity and temperature profiles must be assumed to be similar. It is well known that this is approximately true for a constant-temperature plate, but it is not true for nonisothermal heat transfer. To avoid this assumption it is necessary to use the energy equation in differential form and to solve directly for the temperature profiles. This has been done in the present differential analysis. The heat-transfer rates may then be determined from the slope at the wall, and the result may be written as

$$\frac{St}{St_T} = 1 + \sum_{n=1}^{\infty} C_n \left(\frac{l}{x}\right)^{\lambda_n} \quad (8)$$

where C_n and λ_n are expansion coefficients and eigenvalues, respectively. The differential analysis is not in as good agreement with the experimental data as the integral analysis, but it does allow prediction of the temperature profiles and thus is of interest.

Recently Ferrari (ref. 7) has made a similar differential analysis, except that he allowed for a sublayer. Ferrari included compressibility effects, fluid-property variations, and Prandtl number effects, and thus his is probably the most advanced analysis available at the present time. However, for incompressible flow, Ferrari's result reduces to the result of the present integral analysis (eq. (7)), which is obtained far more easily.

In addition to the several analyses, two empirical correction formulas have been proposed. Maisel and Sherwood (ref. 11) made mass-transfer measurements from a flat plate, and Klein and Tribus (ref. 12) examined their data and proposed the empirical relation

$$\frac{St}{St_T} = \left[1 - \left(\frac{l}{x}\right)^{0.8} \right]^{-0.11} \quad (9)$$

Note that this equation is quite similar to the result of the present integral analysis. Jacob and Dow (ref. 13) made mean heat-transfer measurements on a cylinder in axial flow and found that the correlation of their mean heat-transfer data implied the local Stanton number could be given by

$$\frac{St}{St_T} = 0.8 + 0.2\left(\frac{l}{x}\right) - 0.78\left(\frac{l}{x}\right)^{2.75} + 1.18\left(\frac{l}{x}\right)^{3.75} \quad (10)$$

These empirical equations are in fair agreement with the present data.

Integral Analysis

The momentum equation for the incompressible boundary layer on a flat plate may be written in the following form (see appendix D of ref. 1):

$$\frac{\tau_{bl}(x,y)}{\rho u_\infty^2} = \frac{d}{dx} \int_0^\delta \frac{u}{u_\infty} \left(1 - \frac{u}{u_\infty} \right) dy + \frac{d}{dx} \int_0^y \left(\frac{u}{u_\infty} \right)^2 dy - \frac{u}{u_\infty} \frac{d}{dx} \int_0^y \left(\frac{u}{u_\infty} \right) dy \quad (11)$$

Note that for $y = 0$ equation (11) reduces to the more familiar momentum integral equation

$$\frac{C_f}{2} = \frac{\tau_w}{\rho u_\infty^2} = \frac{d}{dx} \int_0^\delta \frac{u}{u_\infty} \left(1 - \frac{u}{u_\infty} \right) dy \quad (11a)$$

Moreover, if y is set equal to δ in equation (11), the correct result, $\tau_{bl}(x,\delta) = 0$, is obtained. Now if it is assumed that the velocity profile may be represented by an expression of the form

$$\frac{u}{u_\infty} = \left(\frac{y}{\delta} \right)^{1/m} \quad (12)$$

the shear-stress distribution in the boundary layer may be determined from equations (11) and (11a) as

$$\frac{\tau_{bz}(x,y)}{\tau_{bz}(x,0)} = 1 - \left(\frac{y}{\delta}\right)^{(2+m)/m} \quad (13)$$

The mechanism for momentum diffusion in the turbulent boundary layer may be described by

$$\frac{\tau_{bz}}{\rho} = \epsilon_M \frac{\partial u}{\partial y} \quad (14)$$

Strictly speaking, equation (14) holds only far away from the wall where the viscous effects are negligible and all the momentum transfer is by turbulent eddies. However, the power profile assumed by equation (12) will have an infinite gradient at the wall, since $m > 1$; if laminar effects were included near the wall, the shear stress would have to be infinite. It is therefore necessary to neglect the laminar terms and construct an eddy diffusivity such that the wall shear stress has its correct value. This is done simply by combining equations (12), (13), and (14):

$$\frac{\epsilon_M}{\nu} = m \frac{C_f}{2} \frac{\delta}{x} \text{Re}_x \left[1 - \left(\frac{y}{\delta}\right)^{(2+m)/m} \right] \left(\frac{y}{\delta}\right)^{(m-1)/m} \quad (15)$$

Note that the eddy diffusivity is zero both at the wall and at the outer edge of the hydraulic boundary layer.

The energy equation for the boundary layer may be written as follows if dissipation is neglected and the temperature difference $t_w - t_\infty$ is assumed constant in the region of interest:

$$\text{St} = \frac{d}{dx} \int_0^{\delta_T} \frac{u}{u_\infty} (1 - \theta) dy \quad (16)$$

The mechanism for turbulent heat diffusion in the boundary layer may be described by

$$\frac{q''_{bz}}{\rho c_p} = -\epsilon_H \frac{\partial t_{bz}}{\partial y} \quad (17)$$

It will now be postulated that the eddy diffusivity for heat is equal to the eddy diffusivity for momentum, which is the familiar Reynolds analogy.

But, since equations (14) and (17) are assumed to hold everywhere in the boundary layer, even near the wall, this postulation implies that the Prandtl number is 1. This is no serious restriction on the analysis, since the result will simply be a correction on the isothermal Stanton number, and the Prandtl number dependence can be later incorporated in the expression for the isothermal Stanton number (3). The final assumption of this analysis is that the temperature profile is similar to the velocity profile, based on its own boundary-layer thickness:

$$\theta = \left(\frac{y}{\delta_T}\right)^{1/m} \quad (18)$$

Note that no other power profile could be used, or the heat flux at the wall would be infinite. Combining (15) and (18) with (17) gives

$$\frac{q_{bT}''}{\rho c_p u_\infty (t_w - t_\infty)} = \frac{C_f}{2} \left[1 - \left(\frac{y}{\delta}\right)^{(2+m)/m} \right] \left(\frac{\delta_T}{\delta}\right)^{-1/m} \quad (19)$$

Setting $y = 0$ in equation (19) gives

$$St = \frac{C_f}{2} \left(\frac{\delta_T}{\delta}\right)^{-1/m} \quad (20)$$

This expression will now be used as the left side of equation (16). Then, for the assumed velocity and temperature profiles,

$$\frac{m}{\delta} \left[\left(\frac{\delta_T}{\delta}\right)^{-1/m} - \left(\frac{\delta_T}{\delta}\right)^{(1/m)+1} \right] \frac{d\delta}{dx} = (m+1) \left(\frac{\delta_T}{\delta}\right)^{1/m} \frac{d(\delta_T/\delta)}{dx} \quad (21)$$

Integration of (21) yields

$$\int_{\delta(l)}^{\delta(x)} \frac{d\delta}{\delta} = \int_0^{\delta_T/\delta} \frac{\frac{m+1}{m} \left(\frac{\delta_T}{\delta}\right)^{2/m}}{1 - \left(\frac{\delta_T}{\delta}\right)^{(2/m)+1}} d\left(\frac{\delta_T}{\delta}\right) \quad (22)$$

where $\delta(l)$ is the hydraulic boundary-layer thickness at $x = l$. The integrations result in

$$\frac{\delta(x)}{\delta(l)} = \left[1 - \left(\frac{\delta_T}{\delta}\right)^{(2+m)/m} \right]^{-(m+1)/(m+2)} \quad (23)$$

which is equivalent to

$$\frac{\delta_T}{\delta} = \left\{ 1 - \left[\frac{\delta(l)}{\delta(x)} \right]^{(m+2)/(m+1)} \right\}^{-1/(2+m)} \quad (23a)$$

It is well known that in the range $10^4 < Re_x < 10^7$ the boundary-layer thickness δ varies as $x^{4/5}$, and thus equation (23a) may be written as

$$\frac{\delta_T}{\delta} = \left[1 - \left(\frac{l}{x} \right)^{4(m+2)/5(m+1)} \right]^{-1/(2+m)} \quad (24)$$

Substituting (24) in (20) gives

$$St = \frac{C_f}{2} \left[1 - \left(\frac{l}{x} \right)^{4(m+2)/5(m+1)} \right]^{-1/(2+m)} \quad (25)$$

Note that, far away from the discontinuity in wall temperature, where $l/x \rightarrow 0$, $St \rightarrow St_T = C_f/2$. Thus, the final result may be written as

$$\frac{St}{St_T} = \left[1 - \left(\frac{l}{x} \right)^{4(m+2)/5(m+1)} \right]^{-1/(2+m)} \quad (26)$$

If m is taken as 7, equation (26) reduces to

$$\frac{St}{St_T} = \left[1 - \left(\frac{l}{x} \right)^{9/10} \right]^{-1/9} \quad (26a)$$

The mean Stanton number at the end of a plate of length L is defined as the mean St over the heated portion of the plate,

$$St_m = \frac{1}{L-l} \int_l^L St(x) dx \quad (27a)$$

From equations (26) and (3) (for $m = 7$),

$$\frac{St_m}{St_T} = \frac{l}{L-l} \left(\frac{l}{L} \right)^{-0.2} \int_1^{L/l} \sigma^{-0.2} \left(1 - \sigma^{-9/10} \right)^{-1/9} d\sigma \quad (27b)$$

The integral is readily evaluated by setting $\sigma^{9/10} = z$, and finally

$$\frac{St_m}{St_T} = \frac{\frac{5}{4} \left(\frac{L}{l}\right)^{2/10} \left[\left(\frac{L}{l}\right)^{9/10} - 1 \right]^{8/9}}{\frac{L}{l} - 1} = P\left(\frac{L}{l}\right) \quad (28)$$

Note that, as $L/l \rightarrow \infty$,

$$\frac{St_m}{St_T} \approx \frac{5}{4} \quad (28a)$$

which is the well-known result for the constant-temperature plate (ref. 14). In equations (27b) to (28a), St_T is to be evaluated at L .

Differential Analysis

The energy equation for the turbulent incompressible boundary layer may be written, neglecting dissipation and assuming that $t_w - t_\infty$ is constant in the range of interest, as

$$u \frac{\partial \theta}{\partial x} + v \frac{\partial \theta}{\partial y} = \frac{\partial}{\partial y} \left(\frac{q_b''}{\rho c_p} \right) \quad (29)$$

Again it is assumed that the heat-transfer mechanism everywhere in the boundary layer is given by equation (17). In this analysis it will again be assumed that the velocity profile may be given by an expression of the form

$$\frac{u}{u_\infty} = \left(\frac{y}{\delta} \right)^{1/m} \quad (m \approx 5 \text{ to } 8) \quad (12)$$

It should be observed that, although the velocity gradient is infinite at the wall, a reasonable answer will be obtained. The continuity equation for incompressible flow is

$$\frac{\partial u}{\partial x} + \frac{\partial v}{\partial y} = 0 \quad (30)$$

Combination of equations (12) and (30) gives

$$\frac{v}{u_\infty} = \frac{1}{m+1} \frac{d\delta}{dx} \left(\frac{y}{\delta} \right)^{(1/m)+1} \quad (31)$$

The eddy diffusivity for heat was calculated for the integral analysis and is, assuming $\epsilon_H = \epsilon_M$,

$$\frac{\epsilon_H}{\nu} = m \frac{C_f}{2} \frac{\delta}{x} \text{Re}_x \left[1 - \left(\frac{y}{\delta} \right)^{(2+m)/m} \right] \left(\frac{y}{\delta} \right)^{(m-1)/m} \quad (15)$$

Note that the assumption $\epsilon_H = \epsilon_M$ everywhere in the boundary layer, including the region near the wall, again implies $\text{Pr} = 1$. Now, if new coordinates

$$\xi = x/l$$

$$\eta = y/\delta$$

are introduced, equation (29) transforms to

$$\frac{u}{u_\infty} \xi \frac{\partial \theta}{\partial \xi} - \frac{u}{u_\infty} \frac{x}{\delta} \frac{d\delta}{dx} \eta \frac{\partial \theta}{\partial \eta} + \frac{v}{u_\infty} \frac{x}{\delta} \frac{\partial \theta}{\partial \eta} = \left(\frac{x}{\delta} \right) \frac{1}{\delta} \frac{\epsilon_H}{u_\infty} \frac{\partial^2 \theta}{\partial \eta^2} + \left(\frac{x}{\delta} \right) \frac{1}{\delta} \frac{\partial \theta}{\partial \eta} \frac{\partial \epsilon_H}{\partial \eta} \frac{1}{u_\infty} \quad (32)$$

Substitution of (12) in (11a) results in

$$\frac{C_f}{2} = \frac{m}{(m+1)(m+2)} \frac{d\delta}{dx} = M \frac{d\delta}{dx} \quad (33)$$

where $M = m/(m+1)(m+2)$. Blasius has proposed that, for turbulent flow over a flat plate, the friction factor and boundary-layer thickness may be related by (see ref. 14)

$$\frac{C_f}{2} = 0.0228 \text{Re}_\delta^{-1/4} \quad (34)$$

which, when combined with (33), leads to

$$\frac{\delta}{x} = (0.0228)^{4/5} (0.8)^{-4/5} M^{-4/5} \text{Re}_x^{-0.2} \quad (35)$$

and

$$\frac{C_f}{2} = (0.0228)^{4/5} (0.8)^{1/5} M^{1/5} \text{Re}_x^{-0.2} \quad (36)$$

Substituting (12), (31), (15), (35), and (36) into (32) gives

$$\eta^{1/m} \xi \frac{\partial \theta}{\partial \xi} + 0.8M(m-1) \left[\eta^{(1/m)+1} - \eta^{-1/m} \right] \frac{\partial \theta}{\partial \eta} = 0.8Mm \left[\eta^{1-(1/m)} - \eta^{2+(1/m)} \right] \frac{\partial^2 \theta}{\partial \eta^2} \quad (37)$$

With the change of coordinates

$$w = \ln \xi$$

$$z = \frac{u}{u_\infty} = \eta^{1/m}$$

equation (37) can be reduced to

$$\frac{\partial \theta}{\partial w} = \frac{0.8M}{m} (z^{-m} - z^2) \frac{\partial^2 \theta}{\partial z^2} \quad (38)$$

This linear parabolic differential equation resembles the equation describing transient heat conduction in a slab, and techniques similar to those used in such problems will be used in its solution. Equation (38) is to be solved in the region $w > 0$ for $0 < z < 1$. The boundary conditions for $\theta(w, z)$ are

$$\left. \begin{aligned} \theta(w, 0) &= 0 \\ \theta(w, 1) &= 1 \end{aligned} \right\} \quad (39)$$

In addition, there is the "initial" condition that the boundary-layer air must be at the free-stream temperature at the start of the heated section; that is,

$$\theta(0, z) = 1 \quad (40)$$

In handling transient conduction problems it is convenient to divide the solution into "transient" and "steady-state" components. The same technique is useful here. The "steady-state" solution is simply the temperature profile far downstream of the temperature discontinuity,

$$\theta_{ss} = \left(\frac{y}{\delta} \right)^{1/m} = z \quad (41)$$

Note that $\theta = z$ satisfies equation (38).

Thus, θ is divided into

$$\theta = z + \Phi(w, z) \quad (42)$$

where $\Phi(w, z)$ is to satisfy

$$\frac{\partial \Phi}{\partial w} = \frac{0.8M}{m} (z^{-m} - z^2) \frac{\partial^2 \Phi}{\partial z^2} \quad (43)$$

subject to the boundary conditions

$$\left. \begin{aligned} \Phi(w, 0) &= 0 \\ \Phi(w, 1) &= 0 \end{aligned} \right\} \quad (44)$$

and the "initial" condition

$$\Phi(0, z) = 1 - z \quad (45)$$

Equation (43) is solved by separation of variables, where it is assumed that

$$\Phi = W(w)Z(z) \quad (46)$$

which leads to

$$\frac{W'}{W} = \frac{0.8M}{m} (z^{-m} - z^2) \frac{Z''}{Z} = -\lambda \quad (47)$$

The resulting differential equation for $W(w)$ is

$$W' = -\lambda W \quad (48)$$

which has the solution

$$W = Ce^{-\lambda w} \quad (49)$$

The differential equation for $Z(z)$ is

$$Z'' + \frac{m}{0.8M(z^{-m} - z^2)} \lambda Z = 0 \quad (50)$$

The transformation $\zeta = z^{m+2}$ reduces equation (50) to

$$\zeta(1-\zeta) \frac{d^2 Z}{d\zeta^2} + \left(\frac{m+1}{m+2}\right) (1-\zeta) \frac{dZ}{d\zeta} + \frac{(m+1)}{(m+2)} \frac{\lambda}{0.8} Z = 0 \quad (51)$$

which has the solutions (ref. 15, p. 178)

$$Z = C_1 F(\alpha, \beta; \gamma; \zeta) + C_2 \zeta^{1-\gamma} F(\alpha-\gamma+1, \beta-\gamma+1; 2-\gamma; \zeta) \quad (52)$$

where

$$\alpha = \frac{-1}{2(m+2)} \left[1 - \sqrt{1 + 5\lambda(m+1)(m+2)} \right]$$

$$\beta = -\frac{1}{2(m+2)} \left[1 + \sqrt{1 + 5\lambda(m+1)(m+2)} \right]$$

$$\gamma = \frac{m+1}{m+2}$$

Now from (44),

$$Z(0) = 0$$

and thus

$$C_1 = 0$$

From (44),

$$Z(1) = 0 = C_2 F(\alpha-\gamma+1, \beta-\gamma+1; 2-\gamma; 1) \quad (53)$$

But it is well known that (ref. 16)

$$F(a, b, c; 1) = \frac{\Gamma(c)\Gamma(c-a-b)}{\Gamma(c-a)\Gamma(c-b)} \quad (54)$$

and thus, from (53), since C_2 is not zero,

$$0 = \frac{\Gamma\left(\frac{m+3}{m+2}\right)\Gamma(1)}{\Gamma\left(\frac{2m+5-B}{2m+2}\right)\Gamma\left(\frac{2m+5+B}{2m+2}\right)} \quad (55)$$

where

$$B = \sqrt{1 + 5\lambda(m+1)(m+2)}$$

Since the gamma function of a negative integer is infinite, the eigenvalues are given by

$$\frac{2m + 5 - B}{2m + 2} = -n + 1 \quad (56)$$

$$n = 1, 2, \dots$$

and thus the eigenvalues are

$$\lambda_n = \frac{[2(n-1)(m+2) + 2m + 5]^2 - 1}{5(m+1)(m+2)} \quad (57)$$

The solution for φ may now be reduced to

$$\varphi = \sum_{n=1}^{\infty} C_n e^{-\lambda_n w} {}_2F_1(n-1+a, -n; a; z^{m+2}) \quad (58)$$

where $a = (m+3)/(m+2)$.

It is now necessary to expand φ as a series of eigenfunctions in order to satisfy the initial condition (45). It may be shown that (ref. 15, p. 225), if Z_j and Z_k are solutions of (50) associated with the eigenvalues λ_j and λ_k , respectively, the solutions Z_j and Z_k have the following orthogonality property:

$$\int_0^1 \frac{1}{z^{-m} - z^2} Z_j Z_k dz = 0 \quad \text{if } j \neq k \quad (59)$$

Thus by multiplying (58) by

$$\frac{1}{z^{-m} - z^2} {}_2F_1(n-1+a, -n; a; z^{m+2})$$

setting $w = 0$, and integrating from $z = 0$ to $z = 1$, the constants C_n may be evaluated as

$$C_n = \frac{\int_0^1 \frac{1-z}{z^{-m} - z^2} {}_2F_1(n-1+a, -n; a; z^{m+2}) dz}{\int_0^1 \frac{z^2 {}_2F_1^2(n-1+a, -n; a; z^{m+2})}{z^{-m} - z^2} dz} \quad (60)$$

Since the second argument of the hypergeometric function is a negative integer, the functions are actually polynomials, and the coefficients may be evaluated by expansion and integration term by term. This has been done for $n = 1, 2, \text{ and } 3$, resulting in

$$C_1 = (a - 1)(a + 1)$$

$$C_2 = \frac{a^2(a - 1)(a + 3)}{4}$$

$$C_3 = \frac{a^2(a - 1)(a + 1)^2(a + 5)}{36}$$

Evaluation of the higher order coefficients is tedious and is best accomplished by numerical methods. This has been done for $m = 5.6$, which applies in the Reynolds number range of the present data, and it was found that

$$C_4 = 0.1110$$

$$C_5 = 0.0940$$

The final solution for $\theta(x/l, y/\delta)$ may be written as

$$\theta = \left(\frac{y}{\delta}\right)^{1/m} \left[1 + \sum_{n=1}^{\infty} C_n \left(\frac{l}{x}\right)^{\lambda_n} G_n\left(\frac{y}{\delta}\right) \right] \quad (61)$$

where

$$G_n\left(\frac{y}{\delta}\right) = F\left[n-1+a, -n; a; \left(\frac{y}{\delta}\right)^{(m+2)/m}\right] \quad (62)$$

The heat-transfer rate may be found by differentiation of (61) and use of (17) at $y = 0$. This results in

$$\frac{St}{St_T} = 1 + \sum_{n=1}^{\infty} C_n \left(\frac{l}{x}\right)^{\lambda_n} \quad (63)$$

The hypergeometric functions of interest in determining the first five eigenfunctions for $m = 5.6$ have been calculated to four decimal places with an IBM 650 digital computer. These functions are given in table I and are shown in figure 1.

RESULTS AND DISCUSSION

Comparison of Analyses with Heat-Transfer Experiments

A heated plate with an active flow length of about 5 feet was used in this investigation. The heated surface consisted of 24 individually heated strips, thermally insulated from each other. Within control limitations, any desired surface temperature or heat-flux distribution could be set up and desired heat-transfer measurements obtained. The experimental apparatus and techniques are described in detail in reference 2.

Eighteen runs were made for which a step wall temperature existed. Data were obtained at flow Reynolds numbers up to 3.5×10^6 , with step Reynolds numbers ranging from 0.5×10^6 to 3×10^6 . These data are presented in table II(a). The discontinuities were quite sharp, and excellent "steps" were obtained. In reducing these data, allowance was made for conduction between the strips within the plate, and this correction was only important for the first heated strip. The experimental Stanton numbers are actually the average Stanton number over each strip, since the strips are of finite flow length. An analysis indicated that the Stanton number at the center of the strip, where the Reynolds number is calculated, does not differ significantly from the average over the strip, the largest difference occurring on the first heated strip, where the average Stanton number exceeds the Stanton number at the strip center by only about 2 percent. For all other strips, the difference is less than 1/2 percent. Analysis indicated that the imperfectness of the discontinuity in the surface temperature reduced the heat transfer on the first heated strip from the abrupt-discontinuity value by about 2 percent and had no appreciable effect on the heat transfer from the strips farther downstream. Since the error in averaging was approximately compensated for by the error due to the step imperfection, no correction was made for either.

The data are shown graphically in figure 2. It can be shown (ref. 17) that an adequate method for considering the influence of temperature-dependent fluid properties for gas flow in both external and internal boundary layers is to evaluate all fluid properties at the free-stream static temperature and then to include all temperature-dependent property effects in a factor $(T_w/T_\infty)^m$, where the exponent m is a function of geometry alone. Examination of the recent results of an analysis of Deissler and Loeffler (ref. 18) indicates that, for the turbulent incompressible boundary layer, the Stanton number varies as $(T_w/T_\infty)^{-0.4}$, other things being equal. Thus the results are presented in the form $St(T_w/T_\infty)^{0.4}$ against Re_x .

Reference 2 shows that heat transfer to air from isothermal plates may be represented by

$$St_T Pr^{0.4} = 0.0296 Re_x^{-0.2} \left(\frac{T_w}{T_\infty} \right)^{-0.4} \quad (3)$$

Equation (3) is plotted in figure 2. The effect of the unheated starting length is considerable (especially near the step, where the data show a correction as large as 50 percent of St_T), and the data gradually approach the isothermal correlation downstream of the wall-temperature discontinuity.

The data are compared with the various analyses in figure 3. The ratio of the local Stanton number to the isothermal Stanton number as given by equation (3) is plotted against the factor $1 - (l/x)^{9/10}$, which allows equation (26a) to be plotted as a straight line with a $-1/9$ slope. The simple analysis that neglects the dependence of heat transfer on the hydraulic boundary layer (4) is high near the step, as is the semiempirical analysis of Rubesin (eq. (5)). The Seban result (eq. (6)) lies parallel to the data but is displaced by the $Pr^{-2/9}$ factor. The integral analysis employing $1/7$ -power profiles (eq. (26a)) is in excellent agreement with the data over the entire range. However, in the Reynolds number range of these tests, the velocity profile is actually closer to a $1/5.6$ -power profile (see fig. 7). The differential analysis for $m = 5.6$ is slightly high near the step because, near the step, most of the thermal effects are confined to the region near the wall, where the assumed velocity profile is least accurate (see fig. 9(a)). Downstream, where the power profile is a good approximation, the differential analysis for $m = 5.6$ is in good agreement with the data. The success of the integral analysis for $m = 7$ probably lies in the fact that the temperature profiles just downstream of the step are considerably "fatter" than the velocity profiles, and thus are actually closer to $1/7$ -power profiles (see figs. 8 and 9).

Since the agreement of the present integral result (eq. (26a)) with the experimental data is so good, equation (26a) is recommended as the best correlation available at the present time for a step temperature distribution in turbulent incompressible flow. The data are shown as correlated by this equation in figure 4. The correlation is excellent over the entire test range.

The data of Scesa (ref. 5) have been correlated in a similar manner, and this correlation is shown in figure 5. Most of Scesa's data were obtained for a double step in the wall temperature, and thus a more complicated correction was necessary. For this reason the "corrected

Nusselt number" is plotted against Re_x , the correction method following the double-step example of reference 3. These data were obtained over a rather limited range, as is indicated by figure 5, and there is considerable scatter in the data. The accuracy of data obtained from the present apparatus is believed to be considerably better than that obtained with Scesa's small plate. This view is substantiated by the presence of less scatter in the present data.

The mean heat-transfer measurements of Jacob and Dow (ref. 13) are compared with the present analysis (eq. (28)) in figure 6. These data were obtained from tests on a cylinder in axial flow, and the Reynolds number was low so that transition effects may have been of some importance. In consideration of these facts, the agreement of these data with equation (28) is believed to be very satisfactory. These data are also presented on the basis of a corrected mean Nusselt number against Re_x .

Comparison of Survey Data with Theoretical Results

Figures 7 and 8 show velocity and temperature profiles obtained for constant wall temperature, as reported in reference 2. The profiles are similar and may be represented very well by a $1/5.6$ -power formula. The apparatus used to obtain these data and the survey data presented herein is described in detail in reference 2.

Temperature surveys with a step wall-temperature distribution were obtained at three points on the plate and at two different velocities for each point. In these tests the first 11 strips were unheated, and the remaining strips were held at constant temperature. The data from these surveys are shown in table II(b) and are compared with the profiles predicted by the differential analysis ($m = 5.6$) in figure 9. In these comparisons the thermal boundary-layer thicknesses were determined in the manner described in reference 2; the conduction thickness δ_T^* was determined by numerical integration of the temperature profile, and the "best power fit" to the data was determined by plotting θ against y on log-log paper. The conduction thickness is related to the thermal boundary-layer thickness for a power profile of the form $\theta = (y/\delta_T)^{1/m}$ by the equation

$$\delta_T = (1 + m)\delta_T^*$$

The values of δ_T determined in this manner were quite close to the 99-percent thicknesses (ref. 2). In determining the thermal boundary-layer thickness from the differential solution, the same techniques were applied.

The surveys closest to the step ($x/l = 1.20$) show why the heat-transfer rates predicted from the differential analysis are not too good near the step. Near the step, most of the thermal effects are confined to the innermost portions of the boundary layer, where the velocity profile assumed for the analysis is least accurate. The predicted and experimental profiles near the step are not in agreement, as is shown by figure 9(a). Farther downstream the predictions are remarkably accurate, as shown by figures 9(b) and (c). These survey data also show why the integral analysis employing $1/7$ -power profiles works so well; the temperature profiles downstream of the temperature discontinuity are much fatter than the velocity profile, and in fact are quite close to being $1/7$ -power profiles. This is probably responsible for the success of the integral analysis with $m = 7$.

CONCLUDING REMARKS

An integral analysis has been obtained that allows calculation of heat transfer from a flat plate with a step wall-temperature distribution (eq. (26a)). The analysis is in excellent agreement with experimental heat-transfer data of the present and earlier investigations. A differential analysis was obtained that allows the prediction of the temperature profiles in the boundary layer downstream of the temperature discontinuity. The predicted profiles are in good agreement with experimental profiles, but the heat-transfer rates predicted by this analysis are slightly high near the temperature step.

The method of handling the heat-transfer rate at the wall used in the integral analysis is unique in that it allows a power profile having an infinite gradient at the wall to be used everywhere in the boundary layer, while still yielding good results. This eliminates cumbersome "patching" of profiles to obtain a finite slope at the wall. The same technique was used in the differential analysis, wherein the energy equation was solved in spite of the infinite velocity and temperature gradients at the wall. It is believed that this method may also be useful in the treatment of more complex problems, such as flows with pressure gradients, since it provides both analytical simplicity and accurate prediction in the cases thus far explored.

The recommended correlation for heat transfer in the case of a step wall temperature is the result of the integral analysis,

$$\frac{St}{St_T} = \left[1 - \left(\frac{l}{x} \right)^{9/10} \right]^{-1/9} \quad (26a)$$

The isothermal Stanton number St_T for incompressible flow may be computed from the relation

$$St_T = 0.0296 Re_x^{-0.2} Pr^{-0.4} \left(\frac{T_w}{T_\infty} \right)^{-0.4} \quad (3)$$

In this relation the fluid properties are to be evaluated at the free-stream static temperature.

Stanford University,
Stanford, Calif., October 22, 1957.

REFERENCES

1. Reynolds, W. C.: Heat Transfer in the Turbulent Incompressible Boundary Layer with Constant and Variable Wall Temperature. Ph.D. Thesis, Stanford Univ., 1957.
2. Reynolds, W. C., Kays, W. M., and Kline, S. J.: Heat Transfer in the Turbulent Incompressible Boundary Layer. I - Constant Wall Temperature. NASA MEMO 12-1-58W, 1958.
3. Reynolds, W. C., Kays, W. M., and Kline, S. J.: Heat Transfer in the Turbulent Incompressible Boundary Layer. III - Arbitrary Wall Temperature and Heat Flux. NASA MEMO 12-3-58W, 1958.
4. Reynolds, W. C., Kays, W. M., and Kline, S. J.: Heat Transfer in the Turbulent Incompressible Boundary Layer. IV - Effect of Location of Transition and Prediction of Heat Transfer in a Known Transition Region. NASA MEMO 12-4-58W, 1958.
5. Scesa, S.: Experimental Investigation of Convective Heat Transfer to Air from a Flat Plate with a Stepwise Discontinuous Surface Temperature. M.S. Thesis, Univ. of Calif., 1951.
6. Rubesin, Morris W.: The Effect of an Arbitrary Surface-Temperature Variation Along a Flat Plate on the Convective Heat Transfer in an Incompressible Turbulent Boundary Layer. NACA TN 2345, 1951.
7. Ferrari, Carlo: Determination of the Heat Transfer Properties of a Turbulent Boundary Layer in the Case of Supersonic Flow When the Temperature Distribution Along the Constraining Wall is Arbitrarily Assigned. Rep. No. CAL/CM-807, Cornell Aero. Lab., Inc., Mar. 1954. (Contract NOrd-14523.)

8. von Kármán, Th.: The Analogy Between Fluid Friction and Heat Transfer. ASME Trans., vol. 61, no. 8, Nov. 1939, pp. 705-710.
9. Schultz-Grunow, F.: New Frictional Resistance Law for Smooth Plates. NACA TM 986, 1941.
10. Colburn, Allan P.: A Method of Correlating Forced Convection Heat Transfer Data and a Comparison with Fluid Friction. Trans. Am. Inst. Chem. Eng., vol. XXIX, 1933, pp. 174-206.
11. Maisel, D. S., and Sherwood, T. K.: Evaporation of Liquids into Turbulent Gas Streams. Chem. Eng. Prog., vol. 46, no. 3, Mar. 1950, pp. 131-138.
12. Klein, John, and Tribus, Myron: Forced Convection from Nonisothermal Surfaces. Eng. Res. Inst., Univ. Michigan, Aug. 1952. (Contract AF 18(600)-51.)
13. Jacob, Max, and Dow, W. M.: Heat Transfer from a Cylindrical Surface to Air in Parallel Flow with and without Unheated Starting Sections. Trans. ASME, vol. 68, no. 2, Feb. 1946, pp. 123-134.
14. Eckert, E. R. G.: Introduction to the Transfer of Heat and Mass. McGraw-Hill Book Co., Inc., 1950, p. 73.
15. Hildebrand, F. B.: Advanced Calculus for Engineers. Prentice-Hall, 1949.
16. Erdelyi, A., Magnus, W., Oberhettinger, F., and Tricomi, F. G.: Higher Transcendental Functions. Vol. 1. McGraw-Hill Book Co., Inc., 1953, p. 61.
17. Kays, W. M.: A Summary of Experiments and Analyses for Gas Flow Heat Transfer and Friction in Circular Tubes. TR-22, Dept. Mech. Eng., Stanford Univ., June 30, 1954. (Contract N6onr 251.)
18. Deissler, R. G., and Loeffler, A. L.: Turbulent Flow and Heat Transfer on a Flat Plate at High Mach Number with Variable Fluid Properties. Paper No. 55-A-133, ASME, 1955.

TABLE I. - HYPERGEOMETRIC FUNCTIONS FOR
STEP-FUNCTION ANALYSIS

$$[F_n(z) = F(n-1+a, -n; a; z); a = (m+3)/(m+2); \\ m = 5.6.]$$

z	F ₁ (z)	F ₂ (z)	F ₃ (z)	F ₄ (z)	F ₅ (z)
0	1.0000	1.0000	1.0000	1.0000	1.0000
.05	.9500	.8250	.6240	.3932	.1571
.10	.9000	.6509	.3219	.0011	-.2318
.15	.8500	.4972	.0871	-.2214	-.3286
.20	.8000	.3572	-.0876	-.3146	-.2591
.25	.7500	.2311	-.2072	-.3146	-.1170
.30	.7000	.1188	-.2797	-.2529	.0322
.35	.6500	.0204	-.3114	-.1569	.1474
.40	.6000	-.0642	-.3087	-.0490	.2079
.45	.5500	-.1349	-.2784	.0526	.2095
.50	.5000	-.1919	-.2269	.1339	.1609
.55	.4500	-.2349	-.1608	.1859	.0791
.60	.4000	-.2642	-.0868	.2035	-.0137
.65	.3500	-.2796	-.0115	.1865	-.0946
.70	.3000	-.2812	.0586	.1389	-.1435
.75	.2500	-.2689	.1169	.0692	-.1472
.80	.2000	-.2428	.1567	-.0095	-.1033
.85	.1500	-.2028	.1716	-.0780	-.0242
.90	.1000	-.1491	.1548	-.1202	.0594
.95	.0500	-.0745	.0134	-.0138	.0123
1.00	0	0	0	0	0

4995

CW-4 back

TABLE II. - EXPERIMENTAL DATA SUMMARY

(a) Heat-transfer data

Strip	y, lb (hr)(sq ft) $\times 10^{-5}$	$\Delta t_{m, op}$	q_w'' Btu (hr)(sq ft)	$\frac{q_w''}{h}$ (hr)(sq ft) ^(OP)	St $\left(\frac{q_w''}{t_c''}\right) \times 10^{-5}$	$Re_x \times 10^{-6}$	g, lb (hr)(sq ft) $\times 10^{-5}$	$\Delta t_{m, op}$	q_w'' Btu (hr)(sq ft)	$\frac{q_w''}{h}$ (hr)(sq ft) ^(OP)	St $\left(\frac{q_w''}{t_c''}\right) \times 10^{-5}$	$Re_x \times 10^{-6}$	
													$Re_x = 0.506 \times 10^6$; $t_c = 73.50^\circ F$; $p_w = 0.0700$ lb/cu ft
2	25.4	0	---	---	---	0.190	53.8	0	---	---	---	0.259	
3	25.4	0	---	---	---	0.324	54.0	2.2	---	---	---	0.429	
4	25.4	2.4	---	---	---	0.445	53.9	21.8	533	24.4	3.00	0.685	
5	25.4	19.8	484	18.40	2.00	0.569	53.9	22.5	456	20.2	2.48	0.743	
6	25.4	19.8	321	16.18	0.85	0.684	53.7	22.4	423	18.90	2.33	0.895	
7	25.4	19.9	534	15.27	0.50	0.805	53.7	22.2	398	17.93	2.24	1.053	
8	25.4	19.8	285	14.40	0.37	0.922	53.5	22.3	386	17.50	2.15	1.200	
9	25.4	20.2	288	14.36	0.45	1.045	53.6	22.3	387	17.54	2.16	1.360	
10	25.5	20.3	282	12.87	0.11	1.168	53.5	22.9	360	15.73	1.96	1.515	
11	25.5	20.3	259	12.59	0.01	1.290	53.5	23.0	346	15.05	1.87	1.670	
12	25.5	20.4	259	12.43	0.01	1.411	53.5	22.8	358	15.75	1.98	1.826	
13	25.5	20.4	252	12.37	0.02	1.529	53.5	22.6	348	15.05	1.87	1.986	
14	25.4	20.5	252	12.29	0.01	1.656	53.5	22.8	345	15.12	1.88	2.14	
15	25.4	20.5	245	11.32	1.96	1.781	53.5	23.0	341	14.53	1.85	2.29	
16	25.5	20.8	242	11.72	1.92	1.900	53.5	23.1	335	14.50	1.80	2.45	
17	25.5	20.8	242	11.73	1.92	2.01	53.5	22.6	329	14.42	1.80	2.61	
18	25.4	20.7	234	11.23	1.86	2.12	53.5	22.8	322	14.12	1.76	2.76	
19	25.4	20.8	235	11.30	1.85	2.25	53.5	23.0	321	13.95	1.74	2.92	
20	25.4	20.8	235	11.16	1.82	2.36	53.4	23.0	325	14.12	1.76	3.07	
21	25.4	20.8	228	10.94	1.80	2.46	53.4	23.4	315	13.47	1.68	3.22	
22	25.4	21.0	210	10.00	1.85	2.60	53.4	23.5	293	12.47	1.56	3.37	
23	25.5	21.2	220	10.38	1.70	1.72	53.5	23.4	295	12.60	1.58	3.53	
$Re_x = 0.509 \times 10^6$; $t_c = 73.70^\circ F$; $p_w = 0.0751$ lb/cu ft							$Re_x = 1.00 \times 10^6$; $t_c = 84.20^\circ F$; $p_w = 0.0736$ lb/cu ft						
2	17.4	0	0	---	---	0.155	29.9	0	0	---	---	0.228	
3	17.4	0	0	---	---	0.220	30.0	0	0	---	---	0.376	
4	17.4	0	0	---	---	0.304	30.0	0	0	---	---	0.513	
5	17.4	0	0	---	---	0.397	30.0	0	0	---	---	0.650	
6	17.4	3.4	---	---	---	0.469	29.9	0	0	---	---	0.788	
7	17.4	21.1	284	14.47	3.23	0.560	29.8	1.9	---	---	---	0.925	
8	17.4	21.4	254	11.80	2.82	0.633	29.9	20.5	429	21.0	2.94	1.069	
9	17.4	21.5	246	11.53	0.76	0.80	29.9	20.8	398	19.14	2.67	1.207	
10	17.4	21.2	216	10.19	2.44	0.94	29.8	20.9	346	16.65	2.33	1.346	
11	17.4	21.5	211	9.47	2.37	2.41	29.7	21.2	331	15.61	2.19	1.479	
12	17.4	21.4	208	9.70	2.42	2.56	29.8	21.2	336	15.95	2.24	1.620	
13	17.4	21.5	203	9.35	2.25	2.26	1.045	29.8	21.4	328	15.53	2.15	1.762
14	17.4	21.4	202	9.45	2.26	2.29	1.126	29.8	21.5	318	14.94	2.10	1.898
15	17.4	21.6	195	9.00	2.15	2.19	1.209	29.8	21.6	312	14.45	2.03	2.04
16	17.4	21.7	196	9.33	2.16	2.19	1.292	29.8	21.6	308	14.26	1.99	2.18
17	17.4	21.5	187	8.70	2.08	2.11	1.375	29.8	21.6	301	14.21	1.99	2.32
18	17.4	21.5	185	8.80	2.06	2.09	1.455	29.8	21.6	294	13.61	1.91	2.45
19	17.4	21.7	191	8.35	2.00	2.06	1.538	29.6	21.9	289	13.44	1.89	2.58
20	17.4	21.7	183	8.42	2.01	2.04	1.618	29.6	21.6	292	13.52	1.91	2.71
21	17.4	21.9	180	8.21	1.97	2.00	1.700	29.5	21.7	283	13.04	1.84	2.84
22	17.4	22.2	171	7.69	1.84	1.88	1.785	29.7	21.9	265	11.97	1.66	3.02
23	17.4	21.2	172	7.75	1.85	1.68	1.667	29.7	22.0	272	12.32	1.73	3.14
$Re_x = 1.00 \times 10^6$; $t_c = 84.10^\circ F$; $p_w = 0.0740$ lb/cu ft							$Re_x = 1.01 \times 10^6$; $t_c = 84.40^\circ F$; $p_w = 0.0758$ lb/cu ft						
2	19.1	0	0	---	---	0.147	25.8	0	0	---	---	0.182	
3	19.2	0	0	---	---	0.241	25.8	0	0	---	---	0.299	
4	19.3	0	0	---	---	0.329	25.7	0	0	---	---	0.425	
5	19.3	0	0	---	---	0.424	25.6	0	0	---	---	0.57	
6	19.1	0	0	---	---	0.505	25.5	0	0	---	---	0.703	
7	19.1	0	0	---	---	0.596	25.5	0	0	---	---	0.851	
8	19.1	0	0	---	---	0.685	25.5	0	0	---	---	1.042	
9	19.2	0	0	---	---	0.775	25.5	2.5	---	---	---	1.248	
10	19.1	0	0	---	---	0.865	25.6	20.0	323	16.17	2.85	1.067	
11	19.1	2.9	---	---	---	0.956	25.5	20.3	284	14.47	2.64	1.167	
12	19.1	17.3	255	14.65	3.20	3.24	1.042	23.5	20.1	281	14.00	2.62	1.280
13	19.2	17.5	225	12.68	0.74	2.78	1.135	23.5	20.4	272	13.55	2.38	1.395
14	19.2	17.9	206	11.61	2.52	2.56	1.227	23.5	20.3	259	12.67	2.31	1.494
15	19.1	17.9	195	10.91	2.38	2.41	1.308	23.5	20.5	253	12.33	2.19	1.603
16	19.4	17.9	190	10.63	2.50	2.53	1.410	23.4	20.6	251	12.16	2.17	1.711
17	19.2	17.8	185	10.52	2.28	2.32	1.492	23.4	20.6	244	11.84	2.09	1.835
18	19.2	18.1	178	9.84	2.14	2.15	1.580	23.6	20.9	231	11.33	2.01	1.950
19	19.2	18.1	178	9.69	2.08	2.11	1.670	23.5	20.5	226	11.02	1.96	2.03
20	19.1	18.0	171	9.52	2.09	2.12	1.750	23.4	20.6	230	11.17	1.96	2.14
21	19.0	18.1	169	9.35	2.05	2.08	1.836	23.5	20.9	230	11.00	1.96	2.25
22	19.2	18.3	160	8.74	1.90	1.92	1.938	23.4	20.7	204	9.67	1.76	2.36
23	19.2	18.5	165	8.92	1.94	1.98	2.03	23.4	20.6	208	10.08	1.80	2.47

4995

TABLE II. - Continued. EXPERIMENTAL DATA SUMMARY

(a) Condensed heat-transfer data

(Pr) _s	$\text{Be}_L = 2.00 \times 10^5; \tau_w = 20.10^\circ \text{F}; \mu_w = 0.0740 \text{ lb/ft}^2$				$\text{Be}_L = 2.00 \times 10^5; \tau_w = 24.80^\circ \text{F}; \mu_w = 0.0740 \text{ lb/ft}^2$			
	$\frac{\text{Pr}}{\text{Pr}_s}$	$\frac{\mu}{\mu_s}$	$\frac{k}{k_s}$	$\frac{\rho}{\rho_s}$	$\frac{\text{Pr}}{\text{Pr}_s}$	$\frac{\mu}{\mu_s}$	$\frac{k}{k_s}$	$\frac{\rho}{\rho_s}$
1	52.2	0	0	-----	-----	-----	-----	-----
2	52.3	0	0	-----	-----	-----	-----	-----
4	52.5	0	0	-----	-----	-----	-----	-----
5	52.6	0	0	-----	-----	-----	-----	-----
7	52.8	0	0	-----	-----	-----	-----	-----
9	53.0	0	0	-----	-----	-----	-----	-----
10	53.1	0	0	-----	-----	-----	-----	-----
11	53.2	0	0	-----	-----	-----	-----	-----
12	53.3	0	0	-----	-----	-----	-----	-----
13	53.4	0	0	-----	-----	-----	-----	-----
14	53.5	0	0	-----	-----	-----	-----	-----
15	53.6	0	0	-----	-----	-----	-----	-----
17	53.8	0	0	-----	-----	-----	-----	-----
19	54.0	0	0	-----	-----	-----	-----	-----
21	54.2	0	0	-----	-----	-----	-----	-----
22	54.3	0	0	-----	-----	-----	-----	-----
23	54.4	0	0	-----	-----	-----	-----	-----
24	54.5	0	0	-----	-----	-----	-----	-----
25	54.6	0	0	-----	-----	-----	-----	-----
26	54.7	0	0	-----	-----	-----	-----	-----
27	54.8	0	0	-----	-----	-----	-----	-----
28	54.9	0	0	-----	-----	-----	-----	-----
29	55.0	0	0	-----	-----	-----	-----	-----
30	55.1	0	0	-----	-----	-----	-----	-----
31	55.2	0	0	-----	-----	-----	-----	-----
32	55.3	0	0	-----	-----	-----	-----	-----
33	55.4	0	0	-----	-----	-----	-----	-----
34	55.5	0	0	-----	-----	-----	-----	-----
35	55.6	0	0	-----	-----	-----	-----	-----
36	55.7	0	0	-----	-----	-----	-----	-----
37	55.8	0	0	-----	-----	-----	-----	-----
38	55.9	0	0	-----	-----	-----	-----	-----
39	56.0	0	0	-----	-----	-----	-----	-----
40	56.1	0	0	-----	-----	-----	-----	-----
41	56.2	0	0	-----	-----	-----	-----	-----
42	56.3	0	0	-----	-----	-----	-----	-----
43	56.4	0	0	-----	-----	-----	-----	-----
44	56.5	0	0	-----	-----	-----	-----	-----
45	56.6	0	0	-----	-----	-----	-----	-----
46	56.7	0	0	-----	-----	-----	-----	-----
47	56.8	0	0	-----	-----	-----	-----	-----
48	56.9	0	0	-----	-----	-----	-----	-----
49	57.0	0	0	-----	-----	-----	-----	-----
50	57.1	0	0	-----	-----	-----	-----	-----
51	57.2	0	0	-----	-----	-----	-----	-----
52	57.3	0	0	-----	-----	-----	-----	-----
53	57.4	0	0	-----	-----	-----	-----	-----
54	57.5	0	0	-----	-----	-----	-----	-----
55	57.6	0	0	-----	-----	-----	-----	-----
56	57.7	0	0	-----	-----	-----	-----	-----
57	57.8	0	0	-----	-----	-----	-----	-----
58	57.9	0	0	-----	-----	-----	-----	-----
59	58.0	0	0	-----	-----	-----	-----	-----
60	58.1	0	0	-----	-----	-----	-----	-----
61	58.2	0	0	-----	-----	-----	-----	-----
62	58.3	0	0	-----	-----	-----	-----	-----
63	58.4	0	0	-----	-----	-----	-----	-----
64	58.5	0	0	-----	-----	-----	-----	-----
65	58.6	0	0	-----	-----	-----	-----	-----
66	58.7	0	0	-----	-----	-----	-----	-----
67	58.8	0	0	-----	-----	-----	-----	-----
68	58.9	0	0	-----	-----	-----	-----	-----
69	59.0	0	0	-----	-----	-----	-----	-----
70	59.1	0	0	-----	-----	-----	-----	-----
71	59.2	0	0	-----	-----	-----	-----	-----
72	59.3	0	0	-----	-----	-----	-----	-----
73	59.4	0	0	-----	-----	-----	-----	-----
74	59.5	0	0	-----	-----	-----	-----	-----
75	59.6	0	0	-----	-----	-----	-----	-----
76	59.7	0	0	-----	-----	-----	-----	-----
77	59.8	0	0	-----	-----	-----	-----	-----
78	59.9	0	0	-----	-----	-----	-----	-----
79	60.0	0	0	-----	-----	-----	-----	-----
80	60.1	0	0	-----	-----	-----	-----	-----
81	60.2	0	0	-----	-----	-----	-----	-----
82	60.3	0	0	-----	-----	-----	-----	-----
83	60.4	0	0	-----	-----	-----	-----	-----
84	60.5	0	0	-----	-----	-----	-----	-----
85	60.6	0	0	-----	-----	-----	-----	-----
86	60.7	0	0	-----	-----	-----	-----	-----
87	60.8	0	0	-----	-----	-----	-----	-----
88	60.9	0	0	-----	-----	-----	-----	-----
89	61.0	0	0	-----	-----	-----	-----	-----
90	61.1	0	0	-----	-----	-----	-----	-----
91	61.2	0	0	-----	-----	-----	-----	-----
92	61.3	0	0	-----	-----	-----	-----	-----
93	61.4	0	0	-----	-----	-----	-----	-----
94	61.5	0	0	-----	-----	-----	-----	-----
95	61.6	0	0	-----	-----	-----	-----	-----
96	61.7	0	0	-----	-----	-----	-----	-----
97	61.8	0	0	-----	-----	-----	-----	-----
98	61.9	0	0	-----	-----	-----	-----	-----
99	62.0	0	0	-----	-----	-----	-----	-----
100	62.1	0	0	-----	-----	-----	-----	-----

TABLE II. - Concluded. EXPERIMENTAL DATA SUMMARY

(b) Temperature survey data

$x/l = 1.20$				$x/l = 1.60$				$x/l = 1.94$			
$Re_x = 0.754 \times 10^6$ $t_w - t_\infty = 23.70^\circ F$		$Re_x = 1.72 \times 10^6$ $t_w - t_\infty = 25.40^\circ F$		$Re_x = 1.006 \times 10^6$ $t_w - t_\infty = 23.20^\circ F$		$Re_x = 2.30 \times 10^6$ $t_w - t_\infty = 25.50^\circ F$		$Re_x = 1.203 \times 10^6$ $t_w - t_\infty = 23.40^\circ F$		$Re_x = 2.787 \times 10^6$ $t_w - t_\infty = 25.70^\circ F$	
y , in.	θ	y , in.	θ	y , in.	θ	y , in.	θ	y , in.	θ	y , in.	θ
0	0	0	0	0	0	0	0	0	0	0	0
.004	.194	.003	.295	.005	.181	.004	.294	.006	.188	.004	.280
.005	.224	.004	.362	.006	.224	.005	.353	.007	.209	.005	.327
.006	.270	.006	.480	.007	.284	.007	.439	.008	.254	.007	.412
.007	.329	.008	.567	.008	.324	.009	.510	.009	.308	.009	.475
.008	.375	.013	.661	.009	.358	.014	.596	.010	.346	.014	.564
.010	.472	.018	.712	.010	.422	.019	.639	.012	.393	.019	.607
.012	.531	.023	.752	.013	.470	.024	.670	.014	.440	.024	.638
.014	.573	.028	.768	.015	.517	.029	.690	.016	.470	.029	.657
.016	.603	.033	.791	.017	.547	.039	.730	.018	.513	.039	.689
.018	.641	.038	.806	.019	.569	.049	.749	.020	.542	.049	.705
.020	.666	.048	.830	.021	.592	.059	.768	.022	.555	.059	.724
.022	.684	.058	.850	.023	.612	.079	.792	.024	.572	.079	.743
.027	.721	.068	.862	.028	.642	.099	.820	.029	.602	.099	.775
.032	.764	.078	.885	.033	.650	.149	.866	.034	.632	.149	.810
.037	.767	.098	.905	.038	.677	.199	.902	.039	.653	.199	.844
.042	.784	.118	.929	.043	.702	.249	.930	.044	.666	.249	.867
.047	.796	.138	.945	.053	.724	.299	.945	.049	.679	.299	.891
.052	.814	.158	.956	.063	.745	.349	.965	.054	.687	.349	.911
.062	.835	.178	.965	.073	.766	.399	.976	.059	.705	.399	.926
.072	.852	.198	.976	.083	.776	.449	.985	.064	.722	.449	.942
.082	.868	.218	.984	.103	.797	.499	.995	.074	.734	.499	.955
.102	.894	.238	.988	.128	.827	.549	1.000	.084	.734	.549	.965
.127	.919	.258	.996	.153	.840	.599	1.000	.104	.765	.599	.974
.152	.940	.278	.996	.178	.866	.649	1.000	.154	.794	.649	.985
.177	.952	.298	1.000	.203	.883	.699	1.000	.204	.824	.699	.989
.202	.970	.318	1.000	.253	.909	.749	1.000	.254	.855	.749	.996
.252	.985	.338	1.000	.303	.931	.799	1.000	.304	.880	.799	1.000
.302	.995			.353	.956			.404	.918		
.352	1.000			.403	.965			.504	.944		
.402	1.000			.453	.977			.604	.974		
.452	1.000			.503	.991			.704	.987		

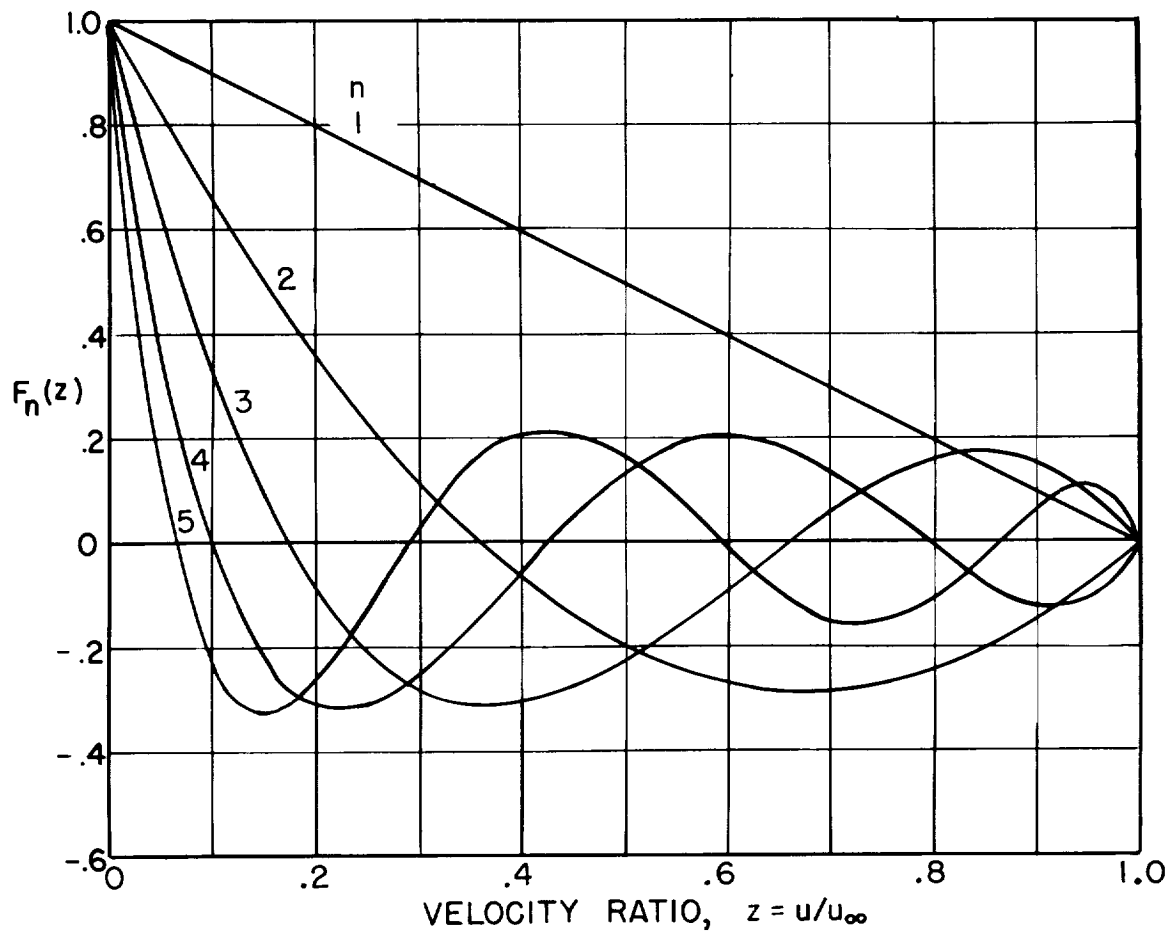


Figure 1. - Hypergeometric functions for step-function analysis.
 $F_n(z) = F(n-1+a, -n; a; z)$; $a = (m+3)/(m+2)$; $m = 5.6$.

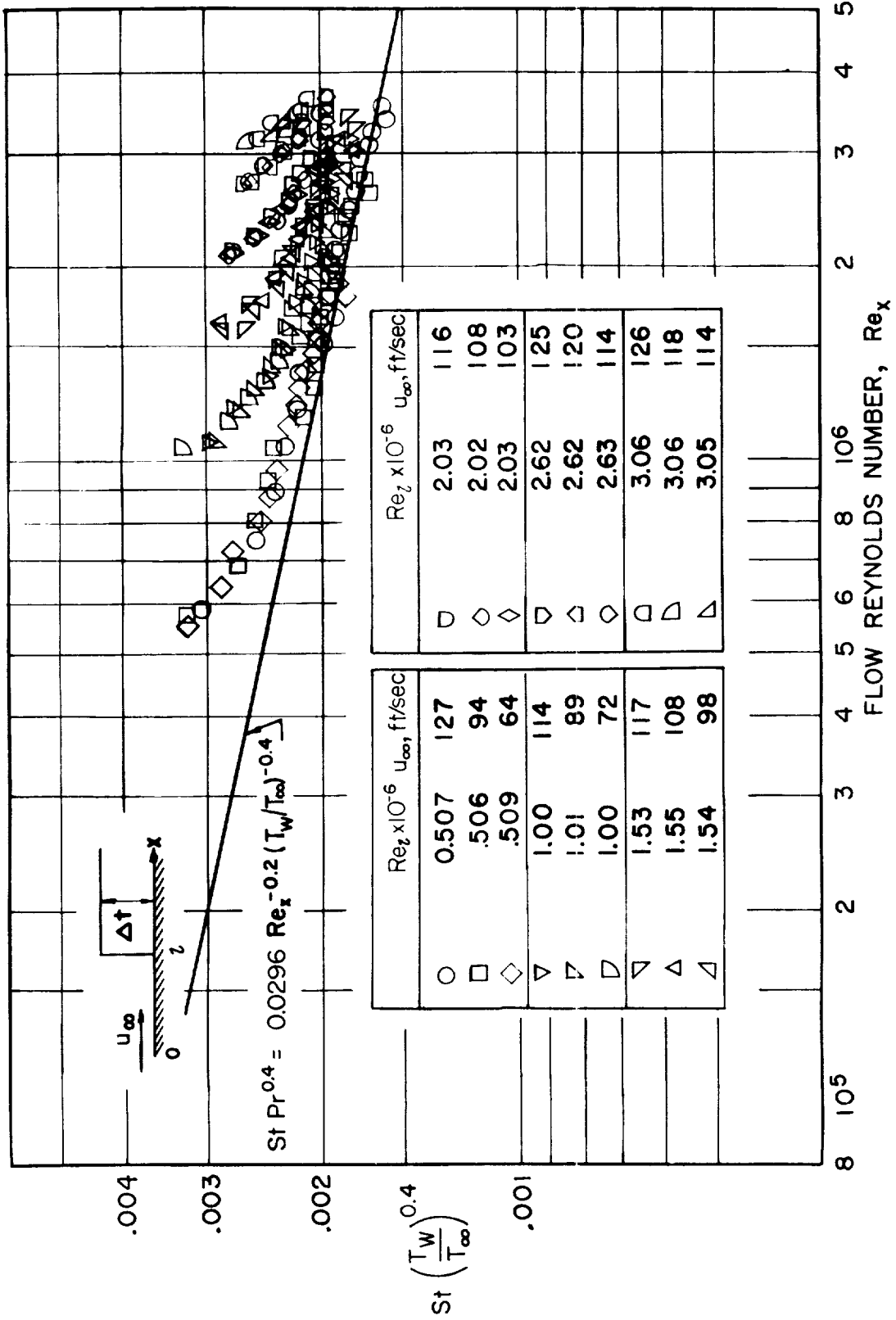


Figure 2. - Local Stanton numbers for step wall-temperature distribution.

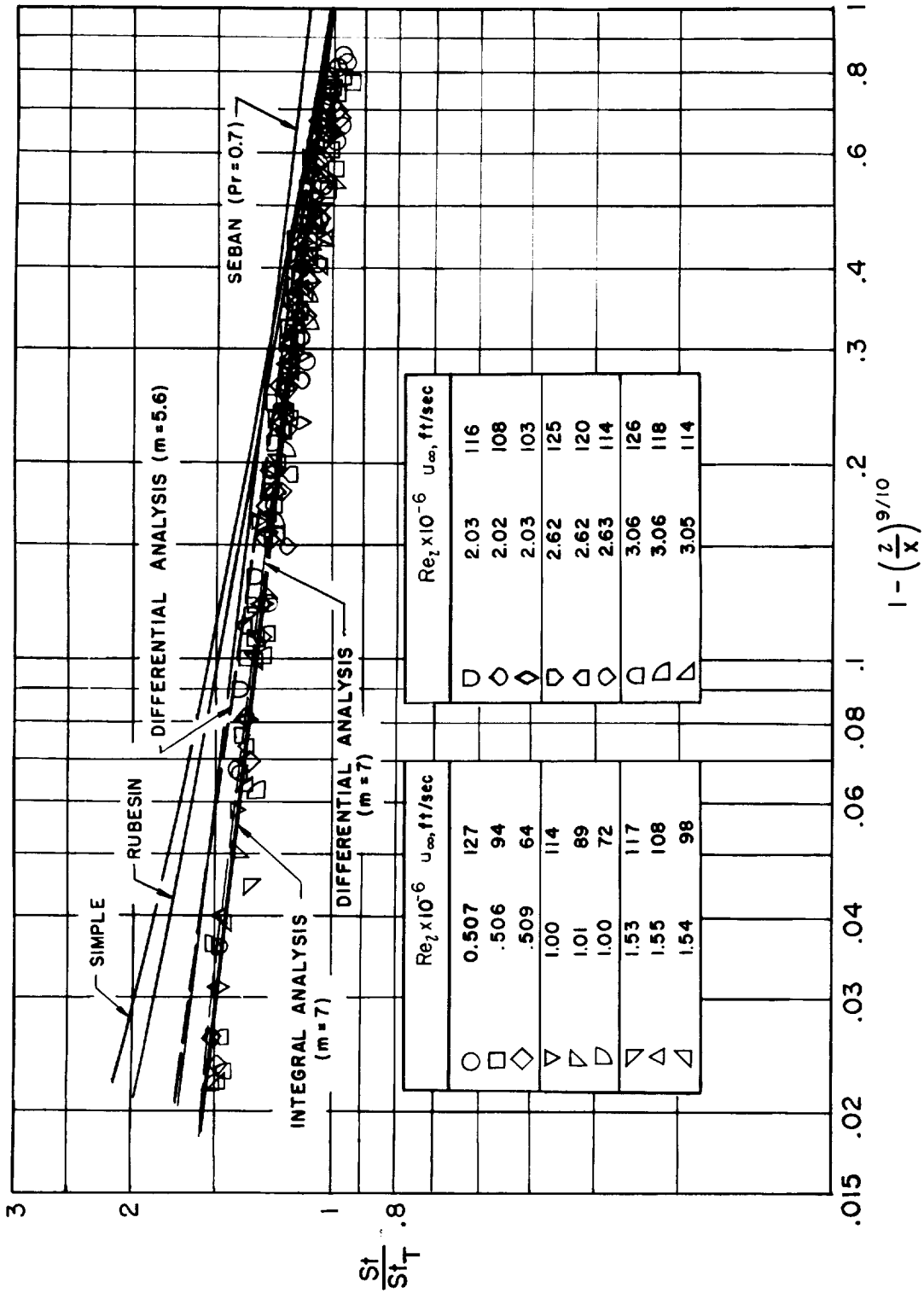


Figure 3. - Comparison of step temperature distribution data with analyses.

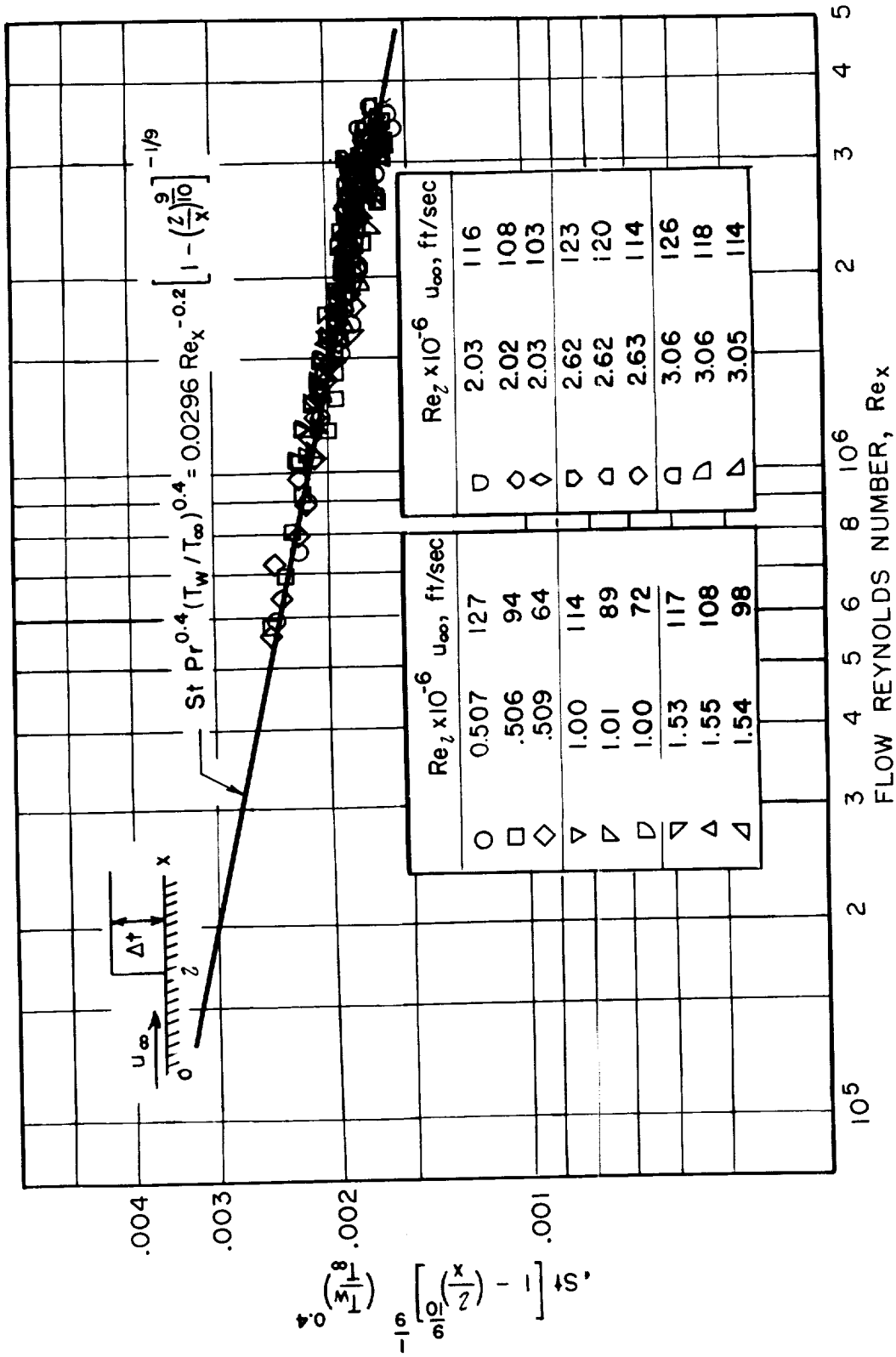


Figure 4. - Local Stanton numbers for step wall-temperature distribution. Prandtl number, 0.7.

4995

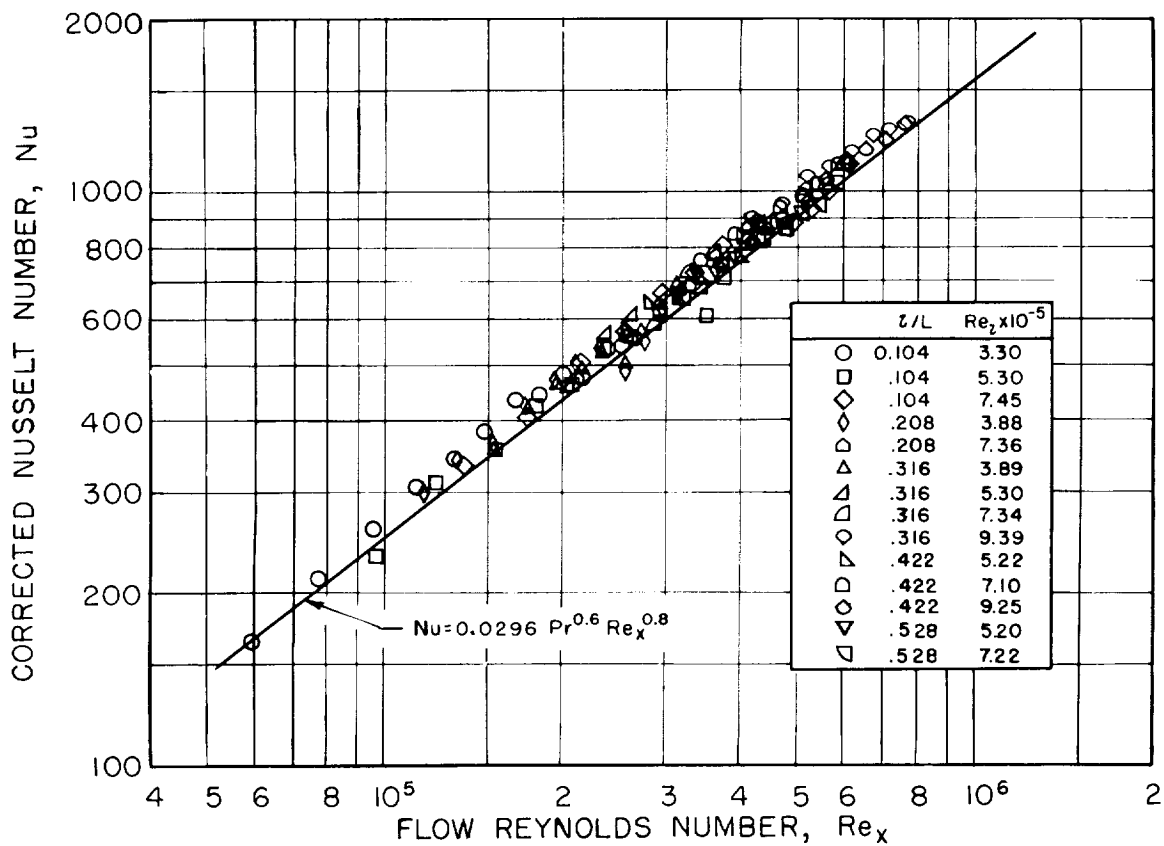


Figure 5. - Comparison of Scesa's data with integral step-function analysis. Prandtl number, 0.71.

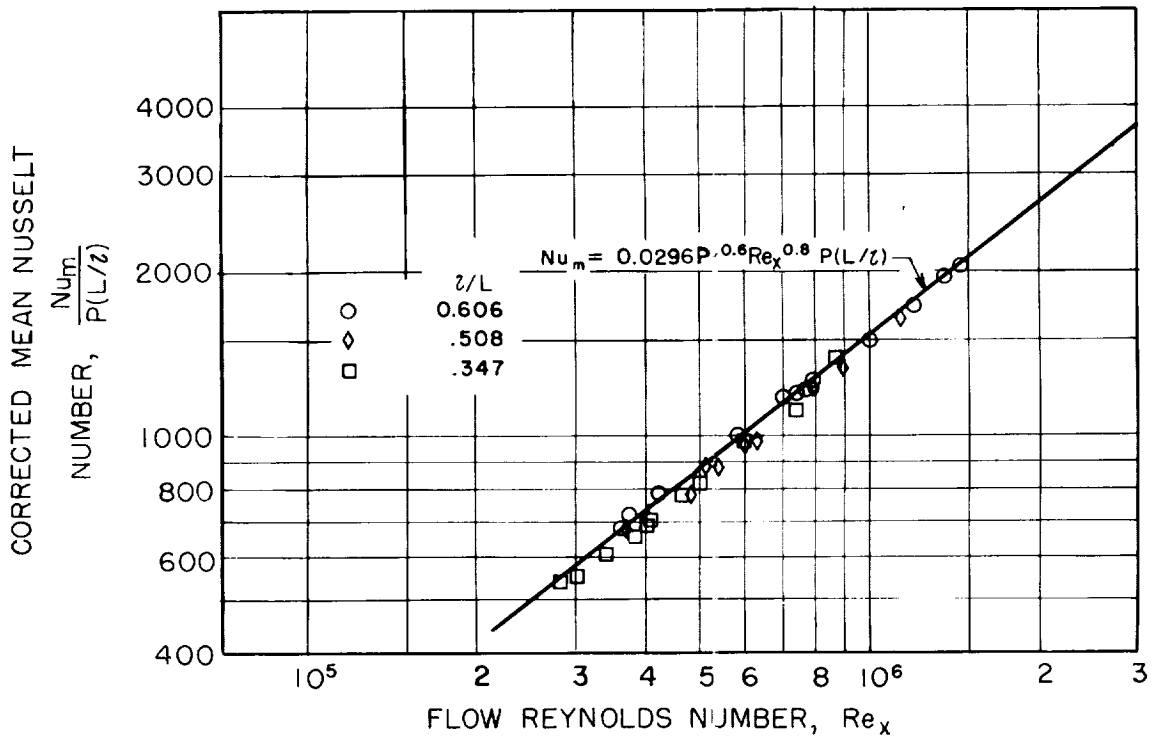


Figure 6. - Comparison of Jacob and Dow's mean heat-transfer data with integral step-function analysis. Prandtl number, 0.71.

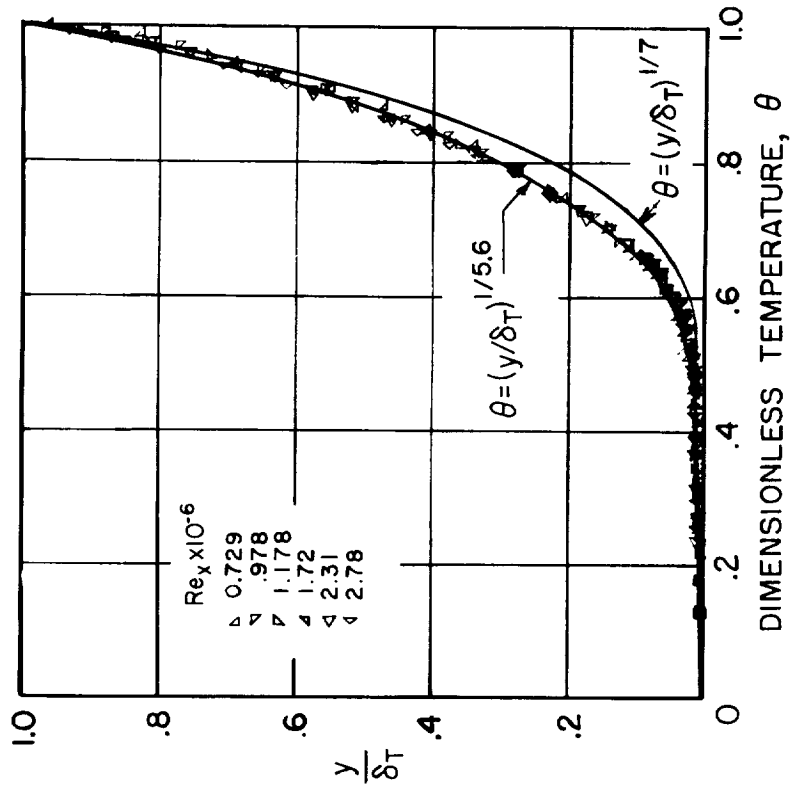


Figure 7. - Velocity profiles (ref. 2).

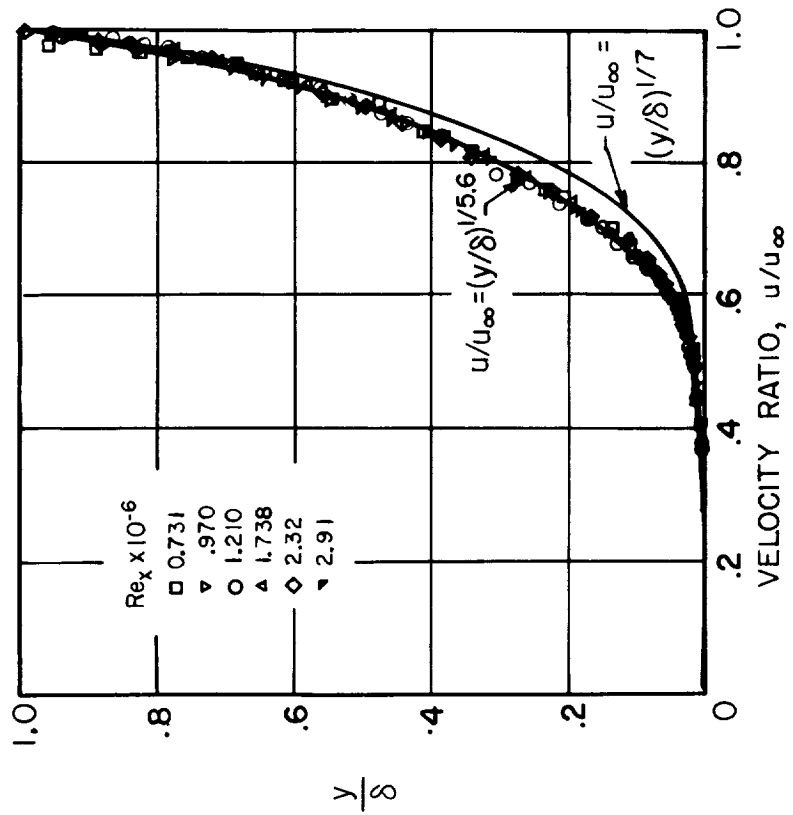
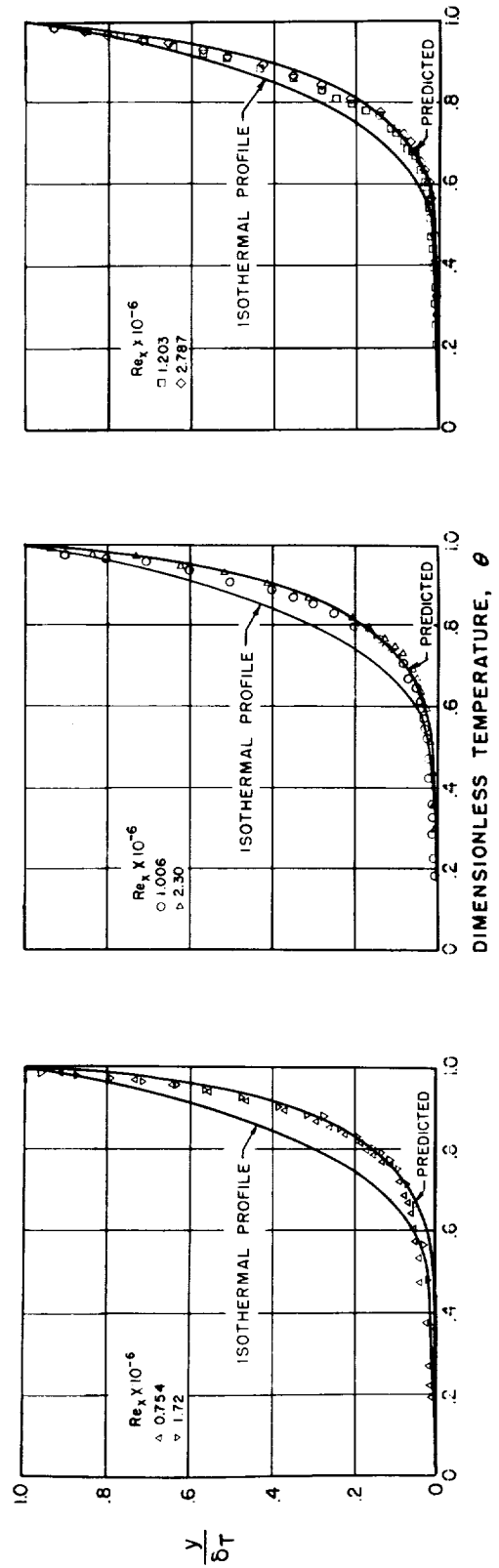


Figure 8. - Temperature profiles for constant wall temperature (ref. 2).



(a) $x/l = 1.20$.

(b) $x/l = 1.60$.

(c) $x/l = 1.94$.

Figure 9. - Temperature profiles for step wall-temperature distribution.